Technical description of radar and optical sensors contributing to joint UK-Australian satellite tracking, data-fusion and cueing experiment

J. D. Eastment, D. N. Ladd and C. J. Walden
STFC Rutherford Appleton Laboratory, Chilbolton Observatory, Drove Road, Chilbolton, Stockbridge, Hampshire, SO20 6BJ, UK.
R. P. Donnelly, A. Ash and N. M. Harwood
Air and Weapons Systems, Defence Science and Technology Laboratory, UK.
C. Smith, J. C. Bennett* and I. Ritchie
EOS Space Systems Pty Ltd., Mount Stromlo Observatory, Cotter Road, Weston Creek 2611, Australia.
* The SPACE Research Centre, School of Mathematical and Geospatial Sciences, RMIT University, GPO Box 2476, Melbourne 3001, Australia.
M. Rutten, N. Gordon and T. Bessell
NSID, Defence Science and Technology Organisation, Australia.

ABSTRACT

The Defence Science and Technology Laboratory (DSTL), Defence Science and Technology Organisation (DSTO), Electro Optic Systems Pty Ltd. (EOS) and the Science and Technology Facilities Council (STFC) have recently participated in a campaign of co-ordinated observations with radar, optical and laser sensors in order to demonstrate and to refine methodologies for orbit determination, data fusion and cross-sensor cueing. The experimental programme is described in detail in the companion paper by Harwood et al., while the results are presented in the paper by Rutten et al. (both in these Proceedings).

At the STFC Chilbolton Observatory in Southern England, the S-band 'Chilbolton Advanced Meteorological Radar' (CAMRa) on a 25 m diameter fully-steerable dish antenna was used to measure object range and radar cross-section.

At the EOS Space Systems facility on Mount Stromlo, near Canberra, Australia, an optical system comprising a 1.8 metre alt / azimuth telescope, fitted with a high-power tracking laser, was used to acquire, lock and laser track the cued objects, providing accurate orbit determinations for each.

DSTO, located at Edinburgh, Australia, operated an optical system consisting of a small commercial telescope and mount, measuring the direction to the objects. Observation times were limited to the evening solar terminator period.

Data from these systems was processed independently, using DSTL-developed and DSTO / EOS-developed algorithms, to perform orbit determination and to cross-cue: (i) the radar, based on the optical and laser measurements; (ii) the optical system, based on the radar measurements; and (iii) the radar, using its own prior observations ('self-cueing'). In some cases, Two Line Elements (TLEs) were used to initialise the orbit determination process; in other cases, the cues were derived entirely from the sensor data. In all 3 scenarios, positive results were obtained for a variety of satellites in low earth orbits, demonstrating the feasibility of the different cue generation techniques.

The purpose of this paper is to describe the technical characteristics of the radar and optical systems used, the modes of operation employed to acquire the observations, and details of the parameters measured and the data formats.

1. INTRODUCTION

The aim of the joint UK-Australian satellite tracking, data-fusion and cueing experiment, described in detail in [1], was to perform co-ordinated tracking of a set of satellite targets with both radar and optical sensors. The objective was to develop observational, analytical and communication procedures which would enable cross-cueing of

geographically separated sensors to acquire designated objects and to perform orbit-determination on them. The analysis of the sensor measurements, and their use to retrieve orbital parameters, is discussed in [2]. Three sensors participated in the campaign, namely the Chilbolton 'CAMRa' radar, the EOS satellite laser ranging (SLR) and optical facility, and DSTO's newly-installed tracking telescope system. The radar and SLR generated observations which were used to produce the cues. The tracking telescope did not produce cueing data, but exploited some of the radar / SLR-generated cues to demonstrate the successful acquisition and tracking of various satellites. The work proceeded in 2 phases. In phase 1, during the week 14/10/2013 – 18/10/2013, the radar was tasked to observe a variety of different satellites of various radar cross-sections and orbital parameters. Based on the results of these observations, and of similar testing at EOS using their SLR and optical systems, a consolidated list of targets was selected which had a high probability of being successfully tracked by both the radar and optical sensors. In phase 2, which ran throughout the weeks 10/02/2014 – 14/02/2014 and 24/02/2014 – 28/02/2014, co-ordinated operations took place with the Chilbolton radar and the EOS SLR facility. A DSTL analyst was based on-site at Chilbolton to facilitate rapid assimilation of the radar data and to perform orbit determination computations. At EOS, another analyst performed the same role using both optical / SLR and radar measurements. During the week 24/02/2014 – 28/02/2014, a number of cuing experiments were attempted. These served to demonstrate (i) cueing of CAMRa by the EOS optical and laser system; (ii) cueing of the EOS optical system by CAMRa; and (iii) 'self-cueing' of future CAMRa observations based on previous radar-only observations. In some cases, NORAD Space-Track TLEs formed an input to the cueing algorithms; in other cases TLEs were not used and the cues relied on sensor observations alone. In the following sections, we describe the technical characteristics of the three systems used in the experiment, and present some examples of their data.

2. CHILBOLTON RADAR

Chilbolton Observatory (Fig. 1) is an outstation of the STFC Rutherford Appleton Laboratory (RAL). It is located near Stockbridge in Hampshire, Southern England (Lat. 51.14446° N, Long. 1.43698° W). The Chilbolton radar, a high-power S-band system equipped with a fully-steerable 25 m diameter dish antenna, has hitherto been used for meteorological and atmospheric science-based research. In 2010, this radar was modified for use as a space surveillance and tracking (SST) asset [3]. During the course of the joint UK-Australian satellite tracking, data-fusion and cueing experiment, 287 satellites passes were observed resulting in 257 successful detections and associated track-files.

Fig. 1. Aerial view of the Chilbolton Observatory site

The 25 m dish, which is the main facility at the Chilbolton site, is shown in Fig. 2. The dish is fully steerable in both azimuth and elevation, and is controlled via a PC-based system. An orbital prediction program generates azimuth and elevation antenna pointing data from TLE sets obtained from the NORAD Space-Track web-site. These data are combined with Network Time Protocol (NTP)-derived time to facilitate real-time programmed tracking. All data were recorded using the specially-modified Chilbolton Advanced Meteorological Radar.

Fig. 2. The 25 m diameter fully-steerable dish

The CAMRa radar is fully described in [4]. For SSA use, it was modified to achieve the specification detailed in Table 1. In this campaign, no *a priori* knowledge of target range (based on the TLE) was used in the signal processing algorithm. Consequently, a pulse repetition frequency (PRF) of 71.428 Hz, corresponding to a pulse repetition interval (PRI) of 14.0 ms and a maximum unambiguous range of 2100 km, was chosen so as to achieve alias-free range measurements for targets in low-earth orbit (LEO). Under these conditions, although the peak power is some 700 kW, the average transmitted power is only 25 W. The system's polariser was configured to transmit pulses of fixed, horizontal polarisation, while the radar's receivers simultaneously recorded both co-polar (horizontal, H) and cross-polar (vertical, V) target returns.

Table 1: Specification of the modified CAMRa radar

Parameter	Value and comments
Operating frequency	3076.5 MHz
Antenna gain	53.5 dBi
Beamwidth	0.28° (FWHM; -3 dB, 1-way)
Polarisation	Tx: H; Rx: H and V
Transmitter type	Cavity magnetron
Peak power	700 kW
Average power	25 W
Pulse repetition frequency	71.428 Hz
Pulse width and coding	0.5 μs, un-coded rectangular
Receiver type	Superhet, log and I/Q channel
Noise figure	3.5 dB, plus duplexing losses (~ 2dB)
IF centre freq. and bandwidth	30 MHz centre, 4 MHz BW
Data acquisition system	7 channels, 12-bit / channel

The theoretical single-pulse signal-to-noise ratio (SNR) as a function of target radar cross-section (RCS) and range (as determined from the standard radar equation) is shown in Table 2.

Table 2: Calculated SNR as a function of RCS and range

RCS / m^2	SNR (dB) at range of 500 km	SNR (dB) at range of 1000 km	SNR (dB) at range of 2000 km
0.1	+9	-3	-15
0.2	+12	+0	-12
0.5	+16	+4	-8
1	+19	+7	-5
2	+22	+10	-2
5	+26	+14	+2
10	+29	+17	+5

The antenna uses an Az / El mount, and can slew up to 1 deg / sec in elevation and up to 3 deg / sec in azimuth. The drive system uses 6 vector drive AC motors: four in azimuth, and two in elevation. Speed and torque control of the motors is achieved by sophisticated servo drive amplifiers. Elevation backlash is minimised by an over-balance condition of the antenna, which ensure the gears are always meshed on one face. The azimuth backlash is minimised by implementation of a torque bias with one motor. Position reference relies on absolute encoders, which can resolve the antenna position to 1/480th (0.002083) of a degree. Position accuracy is verified by tracking radio-stars, such as Cassiopeia A.

Command of the antenna is via an ASCII-coded serial interface. The antenna does not currently utilise a monopulse feed system, hence it cannot use receiver error signals to autotrack. Consequently, programmed tracking is employed. The look-angles required to track specific satellites are computed from TLEs using SDP4 / SGP4 code running in a program called 'predict'. This is an open-source program that is compiled to run under the Linux OS. The version of 'predict' running on the command computer has been modified to output higher-resolution position data. 'predict' operates in server-mode, whereby the data are provided via a TCP/IP interface to the tracking program. Alternatively, it can be run in a command-line mode to prepare the position setpoint files in advance. The velocity setpoint files are prepared by feeding the position setpoint data into a program called 'chobs_trk', which unwinds and shifts the positions into the correct range for the 25 m antenna, then derives the velocities using a polynomial smoothing technique.

Recorded data were stored in NetCDF format, using an adaptation of the scheme normally employed for the meteorological use of this radar. No range-dependent correction has been applied to the signal strengths. Each NetCDF file was post-processed to provide a CCSDS-format TDM (tracking data message) file. The results described here have been derived via a simple scheme in which the target range was identified with the range gate corresponding to the strongest co-polar signal. The value of the co-polar signal strength for the selected gate is included in the TDM file. A limitation of this algorithm is that whenever the target signal momentarily falls, the selected strongest signal will typically correspond to noise in some arbitrary range gate. Further refinement of the algorithm is needed to identify and to remove these spurious values. Range measurements were calibrated by comparison with a readily identifiable terrestrial target (a transmitter mast). The gate containing the maximum co-polar signal was located, and the range offset derived from the difference between the radar-measured range of the gate centre and the known target range (calculated from map references for the radar and the mast using simple trigonometry). The value of this offset was found to be -1.48 km.

Quick-look plots were produced from the TDM files. An example, for the ADEOS satellite, is shown in Fig. 3. The top panel shows the target range identified by the above algorithm. There is one colour-coded dot for each time-stamp in the TDM file, the colours being an indication of co-polar signal strength (in dB). For clarity of presentation, the plotting sequence has been ordered to ensure that stronger signals are plotted in front of weaker ones. The black line corresponds to the predicted target range, as derived from the TLE. The second panel provides a time-series plot of the co-polar signal strength (in blue) as identified by the above algorithm. The red trace is the cross-polar signal for the same range gates. The lower two panels show the time-variation of antenna azimuth and elevation throughout the pass.
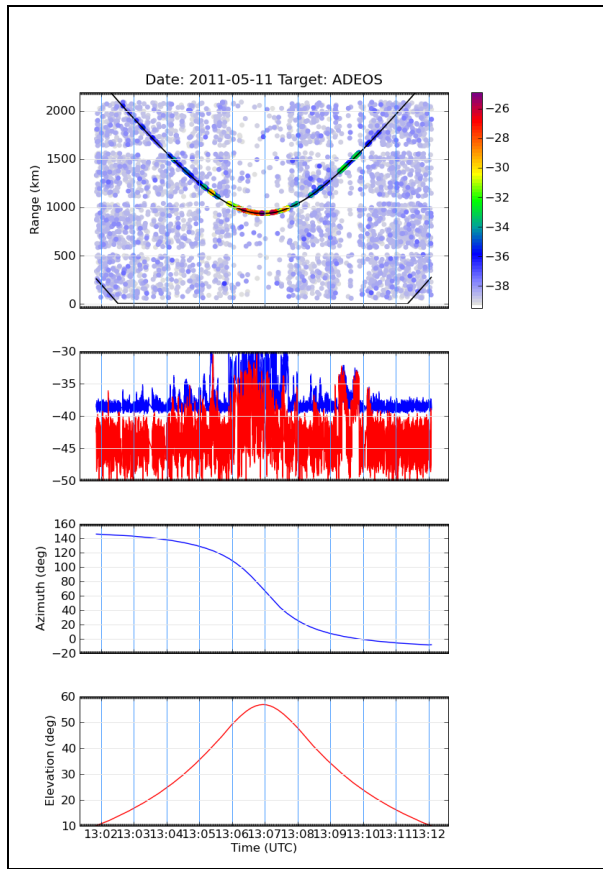
Fig. 3. Quick-look plot for ADEOS satellite pass

3. EOS OPTICAL FACILITY

The experiment's laser ranging activities were performed at the EOS Space Research Centre, located at Mt. Stromlo, near Canberra, Australia (Lat. 35.31630˚ S, Long. 149.00984˚ E). The site is pictured in Fig. 4.

Fig. 4. The EOS Space Research Centre

The facility is currently configured with 1.8 m and 0.35 m telescopes. As shown in Fig. 5, the installation comprises five major sub-systems [5]:

1. Target Acquisition System (TAS) (using the 0.35 m telescope)
2. Beam Locking System (BLS) (using the 1.8 m telescope)
3. High Energy Laser (HEL)
4. Beam Delivery System (BDS)
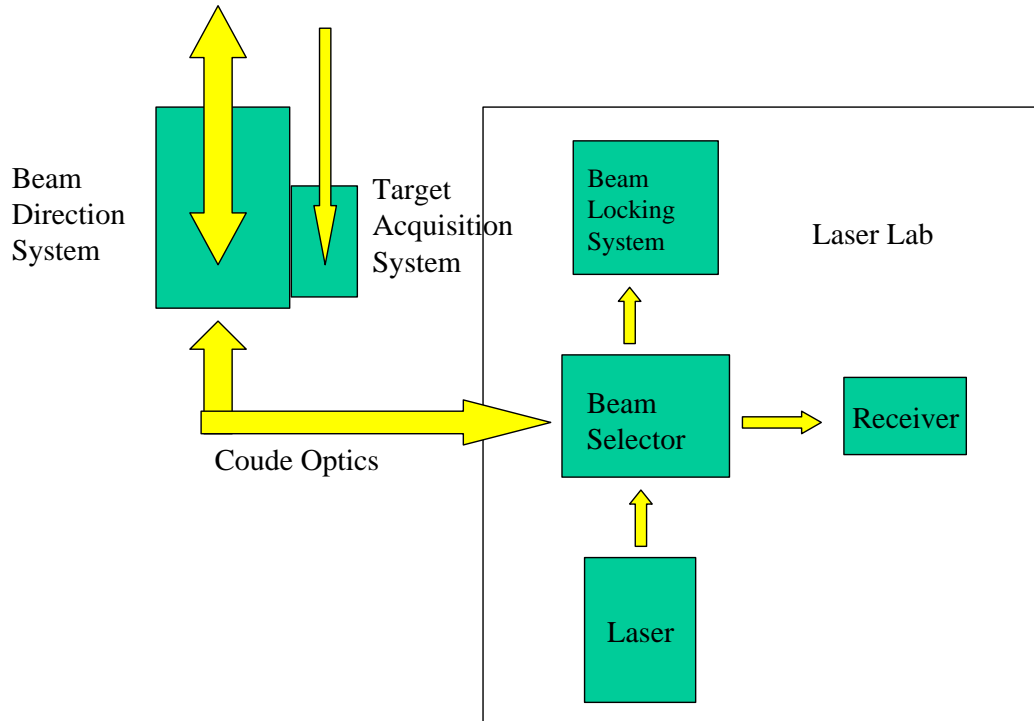5. Ranging Transceiver System (RTS)

Fig. 5. Schematic layout of the optical systems

The TAS is used to detect and center the target in the Beam Locking System field of view (FOV). The TAS uses a 35 cm diameter, f / 0.75, wide-field telescope and high-sensitivity CCD capable of detecting moving objects fainter than 16-17 visual magnitudes, even against the strong Canberra sky background.

The BLS is a high-sensitivity CCD at the end of the 1.8 m telescope Coude path. This camera locks the visible target to the laser boresight with sub-arcsecond accuracy. This camera is able to easily detect all targets seen in the TAS, having the advantage of a 1.8 m diameter collecting area, but has a narrow FOV of ~ 2 arc-minutes diameter on the sky. The BLS camera drives the telescope and fast-steering mirror servo-loops.

Upon initial acquisition, the TAS has control of the telescope tracking servo system, until the target appears in the BLS FOV. At this point, the TAS hands-off to the BLS for fine guiding and beam locking. The BLS also feeds angle data to the Real-Time Orbit (RTO) engine. This system takes angles data from the BLS and re-computes the target orbit in real time, providing more stable target tracking and more lock time with the BLS. The RTO update system uses patented orbital solution algorithms to determine the track of the satellite, and provides an initial distance estimate to the ranging system. The user interface for the TAS and BLS is shown in Fig. 6.
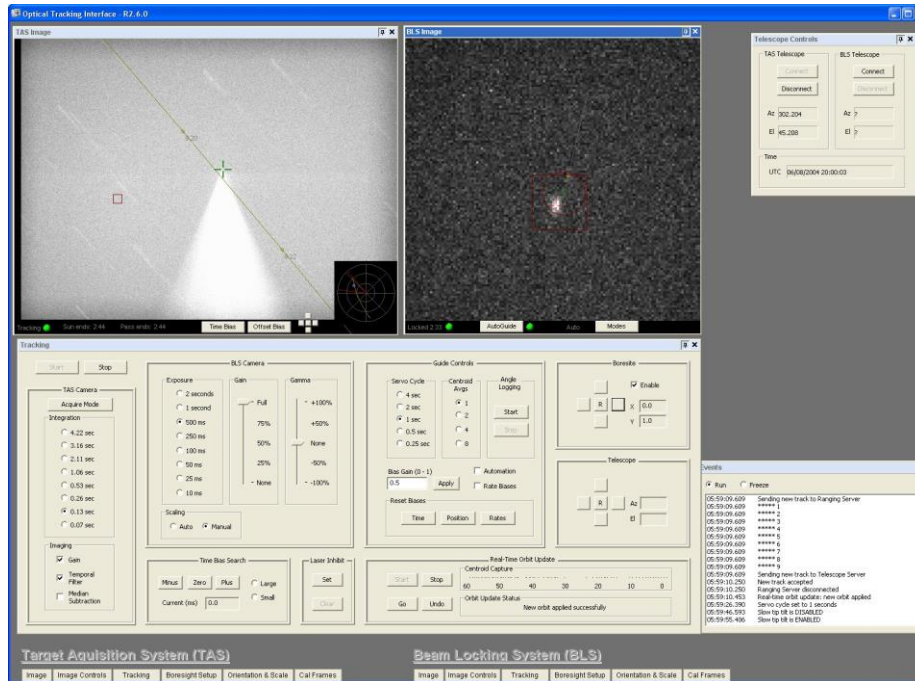
Fig. 6. Typical screen showing the TAS and BLS working in co-operation

The HEL is the main ladar ranging laser. The HEL is a passively mode-locked, diode-pumped Nd:YAG laser, operating at 1.064 μm and providing 200 W average power with 5 ns pulses at 100 Hz. The laser system design was based on a single frequency master oscillator, followed by multi-stage pre-amplifiers and multi-channel power amplifiers. The laser system also incorporates a number of advanced solid-state laser technologies, such as phase-conjugate mirrors and imaging relays for high-energy pulsed lasers.

From the HEL, the beam is expanded-up and then conveyed by the Coude optics to the beam delivery telescope. This is a 1.8 m high-performance telescope in Mersenne (beam expander) configuration, installed in a 9 m co-rotating IceStorm enclosure. The BDS system is configured to provide optimum throughput. It incorporates proprietary coatings and high laser-damage resistance materials, providing minimal degradation of beam quality and high-performance tracking capability for LEO targets.

The beam director telescope is capable of providing absolute pointing of ~ 1.5 arcsec root-mean-square (RMS) anywhere on the sky, and provide tracking (beam pointing stability) to better than 50 milli-arcseconds RMS over any 10 second period. The optical system provides 85 nm RMS wavefronts, though beam projection is limited by atmospheric turbulence. The beam quality degradation by the atmosphere is minimized by careful control of the thermal environment, since any differences between the temperature of the telescope optics and the air can lead to thermal plumes causing air turbulence. The telescope and enclosure minimise these effects by ensuring that air is able to flow through the enclosure and across the telescope. The enclosure is insulated to minimize daytime heating and all of the telescope optics are of light-weight design, so as to ensure they are able to rapidly track ambient temperature changes.

The telescope is of an afocal configuration, and transports the laser beam from the laser laboratory through a series of flat (Coude) mirrors. The mirrors use coatings that provide high reflectivity (99.9%) over a broad wavelength range and a high damage threshold at the laser's operating wavelength.

The RTS provides transmit and receive multiplexing, as well as time-of-flight measurements for the ranging pulses. The timing system provides an accuracy of ~10 pico-seconds RMS. The detectors are sufficiently sensitive to register a single returned photon from each laser pulse.
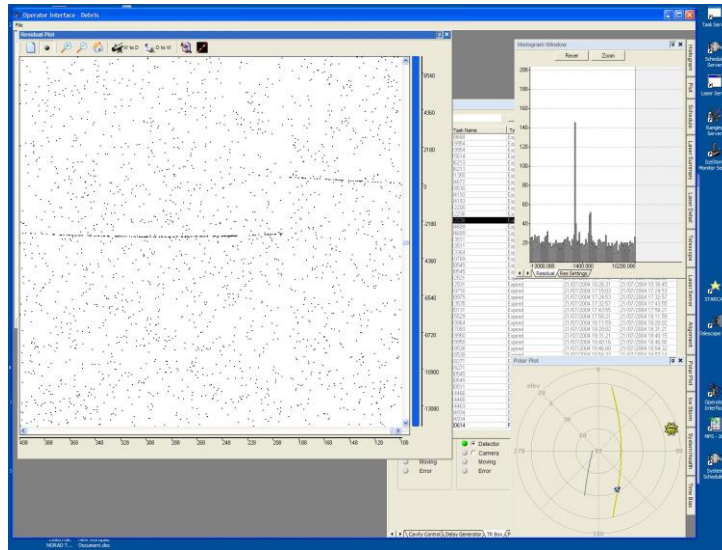
Fig. 7. Typical track output from the RTS showing target trajectory, telescope position and range residual histogram

The ranging screen (upper left in Fig.7 above) shows the detected photon returns. Each dot represents a single photon detection. The random dots are largely thermal noise in the detector, but the target track is a clear trace through the center of the frame. The axes are time on the horizontal (with 0, or current epoch, at the lower right corner), while the vertical axis shows the range residual, which plots the difference between measured and predicted range to the target (measured in pico-seconds). The discontinuity in the trace shows where a real-time orbit update has been completed, after which it is clear that the range residual is much closer to zero – indicating a significantly improved orbit prediction. The window behind the ranging screen shows the system's autonomous scheduling (behind, in upper right). Here, a whole night's targets are loaded into a schedule and the system tracks each object autonomously in turn.

The overall system performance is in close agreement with link-budget estimates. Tracks of objects as faint as 16 visible magnitudes are achieved, with good active track signal-to-noise ratio. Debris objects less than 10 cm in size can be reliably tracked by the system.

An example of the data format used to exchange angular observations during the cueing experiment is shown in Table 3. The laser range observations were processed, and full-rate MERIT II formatted files were created for each pass collected. The cueing information was delivered in an orbital state file, listing epoch, position and velocity.

Table 3: Example of an EOS angular observation file for the object NORAD ID 21801

```
EOSSSAZEL
91082C  021801782600
20120222105338952820010511031511011172953056
20120222105340138920028601040251011172953056
20120222105347701320145781095261011172953056
20120222105642294524556472075721011172953056
20120222105849934128288391531101011172953056
EOSSSAZEL
91082C  021801782600
20120223110823213220842160909191007782923045
20120223110946275122529341316981007782923045
20120223111142243225527801442581007782923045
20120223111332768280225309855710078782923045
```

4. DSTO TRACKING TELESCOPE

During the campaign, DSTO commissioned and operated a new tracking telescope system, located at Edinburgh, South Australia, Australia (Lat. 34.72833° S, Long. 138.64777° E), as shown in Fig. 8.

The optical tube assembly (OTA) is an Officina Stellare RH200 Telescope with a Finger Lakes Instrumentation (FLI) Proline PL4710 CCD. The telescope has an aperture of 200 mm with an f-ratio of f / 3, resulting in a focal length of 600 mm. The CCD is a back-illuminated 1 k x 1 k mid-band sensor. The OTA and CCD are driven by a Paramount ME II Equatorial Mount. A Symmetricon GPS timing card is triggered from the CCD to provide accurate time measurements.

Since the sensor is a passive optical system, the measurements acquired are angular data. The OTA and CCD give an FOV of 76 x 76 arc-minutes. The Paramount has a maximum slew-rate of 4 degrees per second. The sensitivity of the equipment depends on the length of exposure. However, as the system is currently under development, no quantitative characterisation has been performed as yet.

Fig. 8. DSTO tracking telescope and camera system at Edinburgh, South Australia

The data are stored in Flexible Image Transport System (FITS) format, which contains imagery data as well as meta-data (including exposure time, sensor location, etc.). After plate solving, the FITS file is updated with the right ascension and declination of all detected star streaks and satellite objects. The positions of the satellite objects, along with the accurate time stamp from the GPS timing card, are used as inputs for orbit determination.

In the experiment, data from this sensor were not used to actually generate cues. However, the cues produced by DSTL and EOS were successfully used to point this sensor, and to acquire and track the designated objects. An example of such a track is shown in Fig. 9.

DSTO's future plans call for this sensor to be used for research purposes within the field of SSA. In particular, the aim is to utilize the system to assist in the generation of accurate orbits for objects in the LEO to GEO regimes.
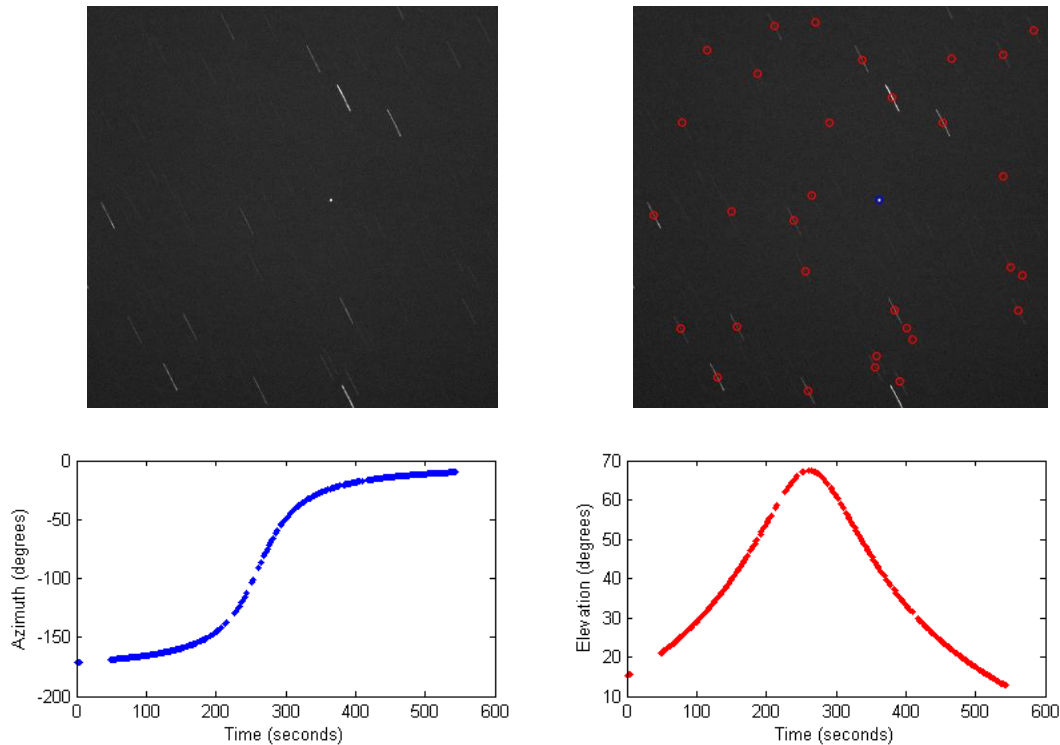
Fig. 9. Example of a satellite detection against background star streaks

5. CONCLUSION

This paper has presented technical details of STFC's radar, EOS's optical / SLR, and DSTO's tracking telescope sensors, all of which contributed to the DSTL-co-ordinated joint UK-Australian satellite tracking, data-fusion and cueing experiment. Aspects of each system's hardware and software have been described, data formats have been discussed, and some examples of sensor observations have been presented.

6. REFERENCES

[1] N. M. Harwood, R. P. Donnelly, A. Ash, M. Rutten, T. Bessell, N. Gordon, J. D. Eastment, D. N. Ladd, C. J. Walden, C. Smith, J. C. Bennett and I. Ritchie, 'Joint UK-Australian space surveillance target tracking, cueing and sensor data fusion experiment'. 'Advanced Maui Optical and Space Surveillance Technologies Conference, AMOS 2014', Wailea Beach Marriott Resort & Spa, 3700 Wailea Alanui, Wailea, Maui, Hawaii, HI 96753.
9 th – 12 th September, 2014.

[2] M. Rutten, N. M. Harwood, J. C. Bennett, R. P. Donnelly, A. Ash, J. D. Eastment, D. N. Ladd, C. J. Walden, N. Gordon, T. Bessell, C. Smith and I. Ritchie, 'Orbit determination analysis for a joint UK-Australian space surveillance experiment'. 'Advanced Maui Optical and Space Surveillance Technologies Conference, AMOS 2014', Wailea Beach Marriott Resort & Spa, 3700 Wailea Alanui, Wailea, Maui, Hawaii, HI 96753.
9 th – 12 th September, 2014.

[3] J. D. Eastment, D. N. Ladd, C. J. Walden and M. L. Trethewey, 'Satellite observations using the Chilbolton radar during the initial ESA 'CO-VI' tracking campaign'. ESA 'European Space Surveillance Conference 2011', INTA Headquarters, Madrid, Spain. Session on 'Radar Observations'. 7 th – 9 th June, 2011. pp 1-8.

[4] J. W. F. Goddard, J. D. Eastment and M. Thurai, 'The Chilbolton Advanced Meteorological Radar: a tool for multidisciplinary atmospheric research'. IEE Electron. and Comms. Engineering Journal, **6**(2), 1994. pp 77-86.

[5] EOS Space Systems Pty Ltd., 'The EOS space debris tracking system'. 30 th June, 2005. pp 1-21.